AIP | The Journal of Chemical Physics

4,4′-, 5,5′-, and 6,6′-dimethyl-2,2′-bipyridyls: The structures, phase transitions, vibrations, and methyl group tunneling of their complexes with chloranilic acid

G. Bator, W. Sawka-Dobrowolska, L. Sobczyk, E. Grech, J. Nowicka-Scheibe et al.

Citation: J. Chem. Phys. **135**, 044509 (2011); doi: 10.1063/1.3613640
View online: http://dx.doi.org/10.1063/1.3613640
View Table of Contents: http://jcp.aip.org/resource/1/JCPSA6/v135/i4
Published by the American Institute of Physics.

4,4′-, 5,5′-, and 6,6′-dimethyl-2,2′-bipyridyls: The structures, phase transitions, vibrations, and methyl group tunneling of their complexes with chloranilic acid

G. Bator,[1,a)] W. Sawka-Dobrowolska,[1] L. Sobczyk,[1] E. Grech,[2] J. Nowicka-Scheibe,[2] A. Pawlukojć,[3] J. Wuttke,[4] J. Baran,[5] and M. Owczarek[1]
[1]*Faculty of Chemistry, University of Wrocław, Joliot-Curie 14, 50-383 Wrocław, Poland*
[2]*Department of Inorganic and Analytical Chemistry, Westpomeranian University of Technology, Piastów 42, 71-065 Szczecin, Poland*
[3]*Institute of Nuclear Chemistry and Technology, Dorodna 16, 03-195 Warsaw, Poland*
[4]*Institut für Festkörperforschung, Forschungszentrum Jülich GmbH, Jülich Centre for Neutron Science at FRM II, Lichtenbergstr. 1, 85747 Garching, Germany*
[5]*Institute of Low Temperature and Structural Research of the PAS, Okólna 2, Wrocław, Poland*

(Received 19 November 2010; accepted 23 June 2011; published online 28 July 2011)

The crystal and molecular structures of 4,4′- and 6,6′-dimethyl-2,2′-bipyridyl complexes with 2,5-dichloro-3,6-dihydroxy-*p*-benzoquinone (chloranilic acid, CLA) have been determined and compared with those of the complex with the 5,5′-derivative, which is known to possess interesting antiferroelectric properties. In the crystalline state, all three compounds form hydrogen bonded chains with N^+–H$\cdots O^-$ and O–H$\cdots$N bridges on both sides of the bipyridyl constituent. The comparison of three derivatives indicates that the N^+–H$\cdots O^-$ hydrogen bonds are shortest for the 5,5′-dimethyl complex. The 4,4′- and 6,6′-derivatives do not show any ferroelectric feature. The 6,6′-one is, however, characterized by a continuous phase transition, revealed in the differential scanning calorimetry, dilatometric, and dielectric characteristics. The tunneling splitting measured by neutron backscattering in the energy range ± 30 μeV for the neat dimethyl bipyridyls and their complexes with CLA indicates that the different splittings are primarily due to the crystal packing effect and that charge transfer between interacting compounds plays only a minor role.
 [doi:10.1063/1.3613640]

I. INTRODUCTION

Both chloranilic acid (CLA) and bipyridyls as well as diazines seem to be interesting compounds from the point of view of crystal engineering due to their disposition of two either proton donor or proton acceptor centers. This can lead to a formation of infinite hydrogen bonded chains. The situation is similar to that observed in the case of squaric acid as the proton donor moiety, which possesses two acidic OH groups. Information about complexes formed by squaric acid can be found in the literature cited in Refs. 1 and 2.

The complex of 5,5′-dimethyl-2,2′-bipyridyl with CLA (5,5′-DMBP$\cdot$CLA) has been described by Kumai *et al.*[3–5] and its dielectric properties appeared to be very interesting. This complex shows an antiferroelectric phase transition related to the proton mediated ordering of molecules. The phase transition has been detected at 318 K. In the high-temperature phase, an asymmetric unit is described by half of the chemical formulas, which includes only one H-bonding site. In the low-temperature structure the asymmetric unit already contains the whole molecule and the low-temperature unit cell is doubled. In the crystal lattice of 5,5′-DMBP$\cdot$CLA, the O–H and N^+–H bonds constitute polar chains along the ***b***-axis. The polarity of the adjacent chains is directed antiparallel; therefore, the bulk crystal lattice symmetry is of antiferroelectric type. The electric permittivity reveals a maximum at the phase transition approaching a value of $\sim$150. The paraelectric-antiferroelectric transition has been assumed to be due to the proton ordering in the strong intermolecular hydrogen bonds. This conclusion is supported by a remarkable isotopic effect – the phase transition temperature is shifted toward high temperature – when proton is substituted by deuterium.

The molecular complex of phenazine with CLA has also been widely investigated.[6,7] The complexes of either tetramethylpyrazine (TMP) (Ref. 8) or dimethylpyrazine (DMP) (Ref. 9) with CLA seem to be objects of some interest. In the case of the TMP$\cdot$CLA complex, one observes a structural phase transition connected with the changes in the hydrogen bond network in the crystal. The lengths of these hydrogen bonds, which link the TMP and CLA molecules, differentiate at low temperature. The complexes formed either between diazines[10] or proton sponge, 2,3,5,6-tetra(2′-pyridyl)pyrazine, and CLA (Ref. 11) also revealed interesting properties.

The aim of the present studies to compare the molecular and crystal structures of the complexes formed by dimethyl-2,2′-bipyridyls with CLA. Since we did not find any crystallographic information file for the structure of the 5,5′-DMBP$\cdot$CLA complex in the Cambridge Structural Database, we decided to reinvestigate its structure at 100 K. In particular, the analysis of the crystal packing with respect to the methyl groups will be performed. The complexation via the charge transfer in the hydrogen bond leads to two effects, a

a)Author to whom correspondence should be addressed. Electronic mail: gb@wchuwr.pl.

change in the environment of the CH_3 groups and a reorganization of the charge distribution. The surrounding of the CH_3 groups is more important, as was shown in several papers.[12–17] This effect causes a change in the rotational potential. However, we also have to take into account another source affecting the dynamics of the CH_3 groups, namely, the charge distribution in the pyridyl rings. The complexation, connected with a charge transfer or strong hydrogen bonding, should lead to a substantial decrease in the electron density around the aromatic ring and a decrease of a barrier to the CH_3 rotations.[15] It seems that the methyl derivatives of bipyridyl can be convenient objects to throw some light on these problems.

The most important aim of this work is, however, an analysis of tunneling of the CH_3 groups at low temperature in the complexes under study. The neutron scattering spectra recorded for the 4,4′-dimethyl-2,2′-bipyridyl with CLA complex at 3.5 K revealed two well shaped peaks assigned to the CH_3 group tunneling. Thus, we decided to investigate the effect of the CH_3 group tunneling on the temperature-dependent infrared spectra of this complex in the wavenumber range assigned to the internal vibrations of molecules with participation of the CH_3 groups as well.

In turn, in a case of the 6,6′-dimethyl-2,2′-bipyridyl with CLA complex, a structural phase transition has been detected at 320 K. It was investigated by means of differential scanning calorimetry (DSC), thermogravimetric and dilatometric methods, as well as by dielectric response in order to determine the possible mechanism of this phase transition.

II. EXPERIMENTAL PART

The complexes of 4,4′-, 5,5′-, and 6,6′-dimethyl-2,2′-bipyridyls with chloranilic acid (4,4′-DMBP · CLA, 5,5′-DMBP · CLA, and 6,6′-DMBP · CLA) were prepared by a slow simultaneous instilling of their solutions in acetone to neat acetone. After instilling, the clear solution was evaporated until a dry precipitate formed. The crystalline complexes were obtained by recrystallization from acetonitrile.

Differential scanning calorimetryruns were recorded using a Perkin Elmer DSC-7 in the temperature range 300–420 K with a scanning rate of 5–20 K/min. The temperature is measured with an accuracy better than 0.1 K (relative error).

The thermogravimetric analysis (TGA) and differential thermal analysis (DTA) measurements were performed on a Setaram SETSYS 16/18 instrument between 290 and 700 K with a ramp rate of 2 K min^{-1}. The scan was performed in flowing nitrogen (flow rate: 1 dm^3 h^{-1}).

The dilatometric measurements were performed by using a thermomechanical analyser Perkin Elmer TMA-7 in the temperature range 300–400 K with a scanning rate of 3 K/min. The dimensions of the sample were of the order of $5 \times 3 \times 1$ mm^3. The error in the thermal expansion measurements is less than 1% (relative error).

The complex dielectric permittivity $\varepsilon^* = \varepsilon' - i\varepsilon''$ was measured with an Agilent 4284A precision *LCR* meter in the frequency range between 300 Hz and 2 MHz and in the temperature range from 300 to 400 K. The dimensions of

TABLE I. Crystal data and structure refinement.

	4,4′-DMBP · CLA	5,5′-DMBP · CLA[a]	6,6′-DMBP · CLA
Formula	C_{18} $H_{14}Cl_2N_2O_4$	C_{18} $H_{14}Cl_2N_2O_4$	C_{18} $H_{14}Cl_2N_2O_4$
Formula weight	393.21	393.21	393.21
T (K)	100(2)	100(2)	100(2)
Crystal system	Monoclinic	Triclinic	Monoclinic
Space group	$P2_1/c$	P-1	$P2_1$
A (Å)	7.832(2)	4.745(1)	4.818(1)
b (Å)	12.147(3)	11.862(2)	11.600(2)
C (Å)	17.521(3)	15.916(3)	15.146(3)
α (°)		111.12(1)	
β (°)	97.90(2)	95.20(1)	90.68(2)
γ (°)		92.33(1)	
V ($Å^3$)	1651.1(7)	829.6(3)	846.4(3)
Z	4	2	2
Crystal size (mm)	$0.30 \times 0.20 \times 0.18$	$0.30 \times 0.25 \times 0.25$	$0.32 \times 0.22 \times 0.20$
θ Range (°)	2.88 to 28.0	2.76 to 28.50	2.21 to 27.50
D_{calc} (g cm^{-3})	1.582	1.574	1.543
Index ranges	$-10 \le h \le 9$	$-5 \le h \le 6$	$-5 \le h \le 6$
	$-16 \le k \le 16$	$-15 \le k \le 15$	$-15 \le k \le 15$
	$-22 \le l \le 22$	$-20 \le l \le 21$	$-19 \le l \le 19$
μ (Mo K_α) (mm^{-1})	0.422	0.420	0.411
No. of reflections collected	24103	11159	12207
No. of independent reflections	3977 ($R_{int} = 0.0219$)	4200 ($R_{int} = 0.038$)	3890 ($R_{int} = 0.025$)
Goodness-of-fit on F^2	1.070	0.984	1.061
Final R_1, wR_2 indices [$F > 4\sigma(F)$]	0.0321, 0.0931	0.0364, 0.0783	0.0295, 0.0734
Final R_1, wR_2 indices (all data)	0.0379, 0.0968	0.0447, 0.0911	0.0347, 0.0756
$\Delta\rho_{max, min}$ (e $Å^{-3}$)	0.227/−0.199	0.30/−0.27	0.277/−0.197

[a]The crystal structure of 5,5′-DMBP · CLA is redetermined in this paper, since the crystallographic data were not available in the Cambridge Crystallographic Data Centre.

the sample were of the order of 5 × 3 × 1 mm^3. The overall error in estimation of the real part of the complex dielectric permittivity value was less than 5%.

The x-ray diffraction data were collected using a KUMA KM4CCD κ-axis four circle diffractometer equipped with an Oxford Cryosystem cooler using graphite monochromated MoK_α radiation. The structures were solved by direct methods with SHELXS-97 program and refined by the full-matrix least-squares methods on all F^2 data using the SHELXL-97 (Ref. 18) program. All non-hydrogen atoms were refined with anisotropic thermal parameters. H atoms attached to O and N atoms were found in a difference Fourier map and refined with isotropic thermal parameters. Other H atoms were treated as riding and their isotropic temperature factors were assumed as 1.2 and 1.5 times U_{eq} of their closest heavy atoms. The crystal data together with experimental and refinement details are given in Table I.

Crystallographic data for the structures reported in this paper (excluding structure factors) have been deposited with the Cambridge Crystallographic Data Centre, CCDC no. 800465-800467.[26]

Infrared spectra of 4,4′-DMBP · CLA, 5,5′-DMBP · CLA, and 6,6′-DMBP · CLA (in KBr pellets) in the temperature range 10–300 K were recorded with an FTIR spectrometer BRUKER IFS-88 over the wavenumber range 4000-400 cm^{-1} with a resolution of 1 cm^{-1}. APD Cryogenics with closed cycle helium cryodyne system was used for temperature-dependent studies. The temperature of the sample was maintained at an accuracy of ±0.1 K. Powder FT-Raman spectra were recorded with an FRA-106 attachment to the Bruker IFS-88 spectrometer over the wavenumber range 3500–80 cm^{-1} at room temperature. The program GRAMS/386 (Galactic Industries) was used for numeric fitting of the experimental data.

High resolution neutron spectra were measured on the backscattering spectrometer SPHERES (Ref. 19) of the Jülich Centre for Neutron Science at Forschungsneutronenquelle Heinz Maier-Leibnitz FRM II (Technische Universität München (TUM), Garching) at temperatures between 3.5 and 40 K in the energy range ±30 μeV. SLAW and FRIDA softwares, available at FRM II, Garching, Germany, were used for fitting the data.

III. RESULTS AND DISCUSSION

A. X-ray structures

The structures of the 4,4′-DMBP · CLA and 6,6′-DMBP · CLA complexes with atom numbering are shown in Figs. 1(a) and 1(b), while the arrangements of the molecules in the crystal lattice are presented in Figs. 2(a) and 2(b). The selected bond lengths and angles are collected in Table II. While 4,4′-DMBP · CLA crystallizes at 100 K in the centrosymmetric monoclinic $P2_1/c$ space group, 6,6′-DMBP · CLA crystallizes in a non-centrosymmetric $P2_1$ one. Fig. 2(a) shows double chains of 4,4′-DMBP · CLA, which are transformed one to other by a center of inversion.

TABLE II. Selected bond lengths (Å) and angles (°).

	4,4′-DMBP · CLA	5,5′-DMBP · CLA	6,6′-DMBP · CLA
CLA^-			
O(2)–C(2)	1.3275(13)	1.329(3)	1.322(3)
O(3)–C(3)	1.2357(13)	1.245(3)	1.248(3)
O(5)–C(5)	1.2641(13)	1.274(3)	1.249(3)
O(6)–C(6)	1.2198(13)	1.228(3)	1.214(3)
C(1)–C(6)	1.4563(16)	1.452(3)	1.445(3)
C(1)–C(2)	1.3482(16)	1.360(3)	1.357(3)
C(2)–C(3)	1.5180(15)	1.536(3)	1.513(3)
C(3)–C(4)	1.4227(15)	1.429(3)	1.405(3)
C(4)–C(5)	1.3883(15)	1.390(3)	1.395(3)
C(5)–C(6)	1.5438(15)	1.557(3)	1.551(3)
$DMPBPH^+$			
N(1)–C(12)	1.3547(14)	1.354(3)	1.365(3)
N(1)–C(16)	1.3434(15)	1.344(3)	1.352(3)
N(2)–C(21)	1.3512(15)	1.362(3)	1.352(3)
N(2)–C(61)	1.3399(15)	1.331(3)	1.346(3)
C(12)–C(21)	1.4920(17)	1.494(3)	1.487(2)
CLA^-			
C(2)–C(1)–C(6)	121.3(1)	120.5(2)	120.8(2)
C(1)–C(2)–C(3)	121.7(1)	122.4(2)	121.4(2)
C(2)–C(3)–C(4)	117.3(1)	117.3(2)	118.3(2)
C(3)–C(4)–C(5)	123.7(1)	122.4(2)	123.6(2)
C(4)-C(5)-C(6)	117.7(1)	119.1(2)	117.0(2)
C(1)–C(6)–C(5)	118.3(1)	118.2(2)	119.0(2)
$DMPBPH^+$			
C(16)–N(1)–C(12)	122.3(1)	123.6(2)	123.8(2)
C(61)–N(2)–C(21)	117.2(1)	118.1(2)	118.6(2)
N(1)–C(12)–C(13)	118.3(1)	117.2(2)	117.9(2)
N(1)–C(12)–C(21)	119.0(1)	119.0(2)	119.0(2)
N(1)–C(16)–C(15)	120.7(1)	121.5(2)	118.3(2)
N(2)–C(21)–C(31)	122.7(1)	122.0(2)	122.6(2)
N(2)–C(21)–C(12)	115.5(1)	115.0(2)	115.6(2)
N(2)–C(21)–C(31)	122.7(1)	122.0(2)	122.6(2)
N(2)–C(61)–C(51)	123.7(1)	124.7(2)	121.8(2)

In all complexes of bipyridyls with CLA, investigated in this paper, one H atom of the CLA hydroxyl group is transferred to the DMBP moiety, to form the CLA^- anion and the $DMBPH^+$ cation. This is supported by the shortening of the corresponding C–O bonds in the chloranilic acid molecules in the low-temperature structure. As the data in Table II show, deprotonation of the OH group in CLA not only substantially shortens its C–O bond (from 1.322(3)–1.329(3) Å to 1.249(3)–1.274(3) Å) but the protonation of the nitrogen atom in bipyridyl also widens the C=N–C angles (from 117.2(1)–118.6(2)° to 122.3(1)–123.8(2)°).

It should be noted that the pattern of the supramolecular arrangement through the hydrogen bondings is similar in all three compounds. The molecular configuration appears to be consistent with the observed geometry in the other salts of the CLA^- monoanion. Therefore, we can state that the molecule in the low-temperature phase belongs to a monovalent form.

The molecules of the DMBP cations are almost planar. The angles between the planes of the two pyridine rings in one DMBP molecule are 4.5(1)°, 2.1(1)°, and 2.4(1)° in 4,4′-DMBP · CLA, 5,5′-DMBP · CLA, and 6,6′-DMBP · CLA,

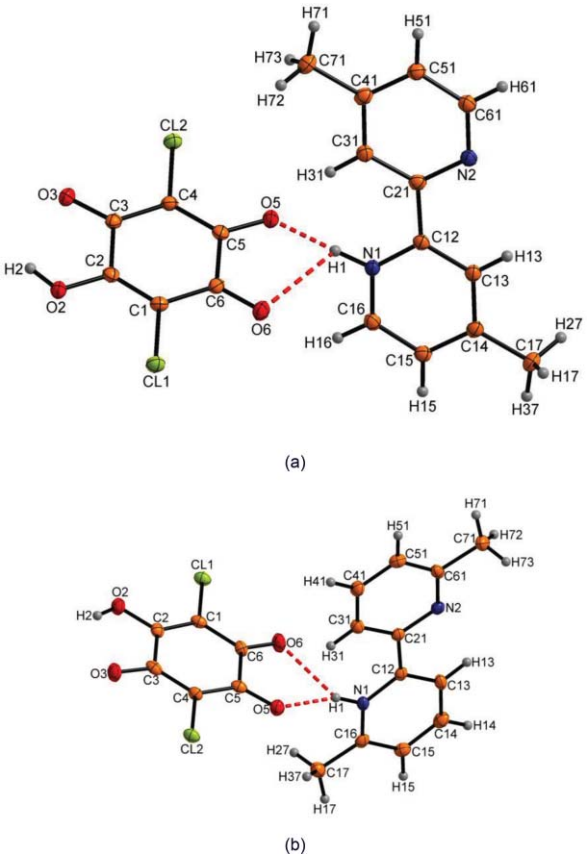

FIG. 1. The independent part of the unit cell with the atom numbering of (a) 4,4′-dimethyl-2,2′-bipyridyl with CLA complex and (b) 6,6′-dimethyl-2,2′-bipyridyl with CLA complex.

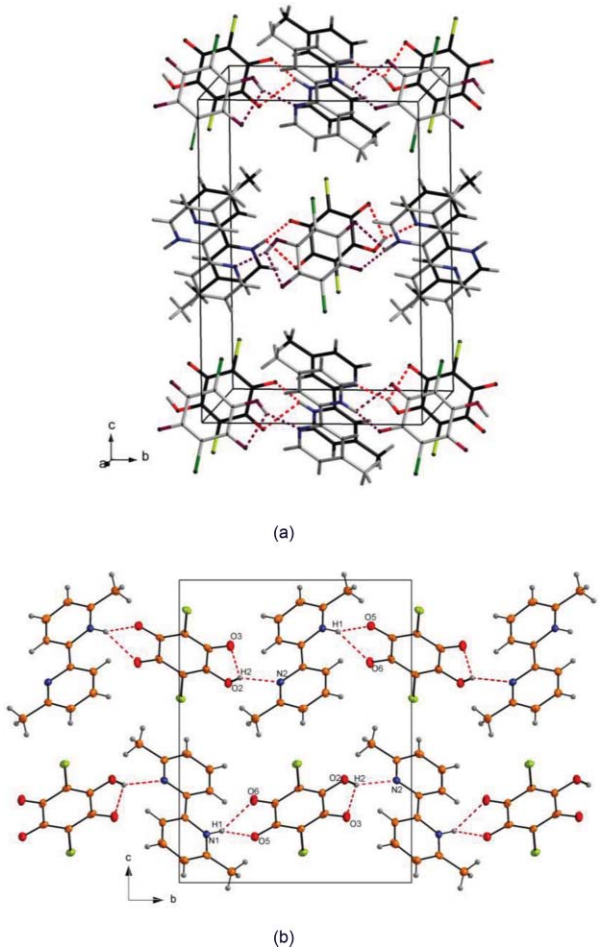

FIG. 2. Crystal packing of (a) 4,4′-dimethyl-2,2′-bipyridyl with CLA complex (gray and black chain polarization vectors are different) and (b) 6,6′-dimethyl-2,2′-bipyridyl with CLA complex along the ***a***-axis at 100 K.

respectively. The methyl groups are essentially coplanar with the pyridine rings. The angles between the plane of the CLA anion and the two individual pyridine rings in the bipyridyl are 53.6(1)° and 53.7(1)° in 4,4′-DMBP · CLA^-, 87.3(1)° and 87.6(1)° in 5,5′-DMBP · CLA, while in the 6,6′-DMBP · CLA they amount to 79.3(1)° and 80.8(2)°.

In all complexes investigated, the two moieties are linked by a bifurcated hydrogen bond of the N(1)–H(1) · · · O(5) and N(1)–H(1) · · · O(6) type as well as by the O(2)–H(2) · · · $N(2)^i$ hydrogen bond (Table III) to form infinite chains running along the ***b***-direction (Figs. 2(a) and 2(b)). The corresponding N(1)–H(1) · · · O(5) and N(1)–H(1) · · · O(6) distances are in the range of 2.569(3)–2.775(3) Å and 2.948(1)–3.069(3) Å, respectively. In turn, the O(2)–H(2) · · · N(2) distances lie in the range of 2.658(3)–2.854(3) Å. Moreover, the crystal packing is stabilized by the C(13)–H(13) · · · O(5) and C(31)–H(31) · · · O(2) interactions as well as by the π-π stacks.

In the crystal of 5,5′-DMBP · CLA the molecules, translated along the [100] direction, are held together by the π-stacking interactions between the pyridyl rings of the adjacent DMBP molecules (with the interplanar and intercentroid distances equal to 3.297 Å and 3.578 Å, respectively). Although, in the case of 6,6′-DMBP · CLA, the bipyridyl cations are also stacked in the same crystallographic direction, the corresponding distances are larger and equal to 3.418 Å and 3.800 Å, respectively.

Centrosymmetrically related molecules of 4,4′-DMBP · CLA also form the π-π stacks. The mean value of the interplanar and intercentroid distances between two pyridyls (symmetry codes: x, y, z and 2 − x, 1 − y, 1 − z) is equal to 3.312 and 3.795 Å, respectively, and between two chloranilic rings (symmetry codes: x, y, z and −x, 1 − y, 1 − z) is 3.390 and 3.781 Å. This indicates rather weak π-π arrangement.

When we compare the intermolecular N^+–H · · · O^- and O–H · · · N hydrogen bonds in 4,4′-DMBP · CLA and 6,6′-DMBP · CLA with those in 5,5′-DMBP · CLA, in which antiferroelectric properties have been found by Kumai *et al.*,[3] we note that they are remarkably shorter in the 5,5′-DMBP · CLA complex (see Table III). This means that 5,5′-DMBP · CLA is unique among these three DMBP · CLA complexes from the point of view of hydrogen bond lengths.

B. Tunneling splitting

To a good first approximation, the dynamics of methyl groups in a molecular crystal can be described as uniaxial rotation of uncoupled rotors in a fluctuating field. This single-particle model has been worked out in much detail in a monograph by Press;[20] it has been found

TABLE III. Hydrogen bonds for 4,4′-DMBP · CLA,[a] 5,5′-DMBP · CLA,[b] and 6,6′-DMBP · CLA.[c]

D–H · · · A (Å)	D–H (Å)	H · · · A (Å)	D · A (Å)	∠ D–H · · · A (°)
4,4′-DMBPH$^+$ · CLA$^-$				
N(1)–H(1) · · · O(5)	0.94(2)	1.74(2)	2.660(1)	166(1)
N(1)–H(1) · · · O(6)	0.94(2)	2.48(2)	2.948(1)	111(1)
O(2)–H(2) · · · O(3)	0.89(2)	2.21(2)	2.662(1)	111(1)
O(2)–H(2) · · · N(2)^{i}	0.89(2)	1.96(2)	2.778(1)	153(2)
C(31)–H(31) · · · O(5)	0.93	2.29	3.151(2)	153
C(13)–H(13) · · · O(2)^{ii}	0.93	2.41	3.138(2)	165
5,5′-DMBPH$^+$ · CLA				
N(1)–H(1) · · · O(5)	0.85(3)	1.78(3)	2.569(3)	154(3)
N(1)-H(1) · · · O(6)	0.85(3)	2.50(3)	3.069(3)	125(3)
O(2)–H(2) · · · O(3)	0.83(3)	2.27(3)	2.702(2)	113(3)
O(2)–H(2) · · · N(2)^{i}	0.83(3)	1.91(3)	2.658(3)	150(3)
C(31)–H(31) · · · O(5)	0.93	2.40	3.241(3)	150
C(13)–H(13) · · · O(2)^{ii}	0.93	2.59	3.456(3)	156
6,6′-DMBPH$^+$ · CLA$^-$				
N(1)–H(1) · · · O(5)	0.92(2)	1.89(2)	2.775(3)	161(2)
N(1)–H(1) · · · O(6)	0.92(2)	2.46(2)	2.976(3)	116(2)
O(2)–H(2) · · · O(3)	0.82(3)	2.15(2)	2.633(2)	118(2)
O(2)–H(2) · · · N(2)^{i}	0.82(3)	2.13(3)	2.854(3)	147(2)
C(31)–H(31) · · · O(5)	0.93	2.35	3.259(3)	166
C(13)–H(13) · · · O(2)^{ii}	0.93	2.47	3.378(3)	167

[a]Symmetry code for 4,4′-DMBP · CLA: (^{i}) x, y − 1, z, (^{ii}) x, y + 1, z.
[b]Symmetry code for 5,5′-DMBP · CLA: (^{i}) x, y + 1, z, (^{ii}) x, y − 1, z.
[c]Symmetry code for 6,6′-DMBP · CLA: (^{i}) x, y + 1, z, (^{ii}) x, y − 1, z.

adequate for the description of experimental data in numerous compounds.[21]

The methyl group moves in a potential $V(\phi)$, where ϕ is a one-dimensional angular coordinate. Following Prager and Heidemann,[21] this potential consists of a static and a fluctuating part, $V(\phi) = V_{st}(\phi) + V_{fl}(\phi,t,T)$ (t stands for time and T – temperature). V_{st} is the mean electrostatic potential caused by the crystalline environment in the low-temperature limit; V_{fl} accounts for the fluctuations of this environment mainly caused by phonons and by rotations of neighboring methyl groups.

The magnitude of V_{st} and V_{fl} must be set in relation to the rotational constant $B = \hbar^2/2I$ (= 0.67 ± 0.006 meV, I: moment of inertia). In almost all cases, the static potential is *strong*: $|\bar{V}_{st}| \gg$ B. Consequently, the methyl groups cannot rotate freely; they are basically confined to *pocket states* around the potential minima. At low temperatures, the fluctuating potential is *weak*: $|\bar{V}_{st}| \ll$ B. In this case, the threefold degeneracy of the pocket ground state is lifted by quantum tunneling. In the high-temperature limit, the fluctuating potential is *strong*: $|\bar{V}_{fl}| \gg$ B. In this case, transitions between pocket states are achieved by thermally activated jumps.

In dimethylbipyridyls, we have two inequivalent methyl positions (n = 1, 2), and for each of them the crystal field has no particular symmetry so that the potentials $V_n(\phi)$ have only the $2\pi/3$ periodicity required by the threefold symmetry of the methyl groups. This leads[20,21] to the scattering function,

$$S(Q,\omega) = \left(2\left(\frac{5}{3} + \frac{4}{3}j_o(Qd)\right) + r(Q)\right)\delta(\omega) + \sum_{n=1}^{2}\left(\frac{2}{3} - \frac{2}{3}j_o(Qd)\right)\{\delta(\omega+\omega_{tn}) + \delta(\omega-\omega_{tn})\}, \quad (1)$$

with momentum transfer $\hbar Q$ and energy transfer $\hbar\omega$. On the right-hand side, d is the H–H distance in the methyl group, and $\hbar\omega_t$ is the ground state tunnel splitting. The term $r(Q)$ stands for the elastic scattering by the rest of the molecule. It is dominated by incoherent scattering from the seven non-methyl protons; therefore, in first approximation, $r(Q) \approx 7$. For fully resolved tunneling bands, Eq. (1) implies an intensity ratio,

$$\frac{I_{inel}}{I_{el}} = \frac{4 - 4j_o}{10 + 8j_o + 3r}, \quad (2)$$

which shall be compared to the experiment below.

At higher temperatures, thermal fluctuations of the lattice become significant causing a softening and a broadening of the tunneling transitions. The frequencies $\omega_{tn}(T)$ become temperature dependent, and the Dirac distributions in Eq. (1) must be replaced by Lorentzians with linewidth $\Gamma_n(T)$. It is now well established[16,21,22] that an Arrhenius expression provides a reasonable first approximation for the broadening,

$$\Gamma_n = \Gamma_{on}\exp\left(\frac{E_{\Gamma n}}{kT}\right), \quad (3)$$

and for the softening,

$$\hbar\omega_n = \hbar\omega_n(T=0)\left[1 - A_n^{\sin}\exp\left(\frac{E_n^{\sin}}{kT}\right)\right]. \quad (4)$$

The activation energies $E_{\Gamma n}$ represent the distance from the pocket ground state to the first librational level. The sinusoidal coupling coefficients $A_n^{\sin}$ and the activation energies $E_n^{\sin}$ describe the interaction between the methyl group and the heat bath.

High-resolution inelastic neutron scattering was used to obtain $S(Q, \omega)$ for the three pure components (substituted bipyridyls) as well as for their three complexes with CLA. The measurements were carried out in the temperature range between 3.5 and 40 K.

Some tunneling spectra of neat 4,4′-DMBP as well as for its complex 4,4′-DMBP · CLA at several temperatures between 3.5 and 40 K in the energy range ±14 μeV for neat 4,4′-DMBP and in the energy range ±4 μeV for the 4,4′-DMBP · CLA complex are depicted in Fig. 3.

Solid lines are fits with the standard model described above, consisting of a Dirac component for the elastic scattering and Lorentzians for the tunneling excitations; the theoretical curve has been convoluted with the instrumental resolution function.

From the temperature dependence of the positions, $\Delta E_i = \hbar\omega_i(T=0) - \hbar\omega_i$, we have estimated the E_{01} value using Eq. (4). The Arrhenius plot is shown in Fig. 4 for the 4,4′-dimethyl-2,2′-bipyridyl with CLA as an example.

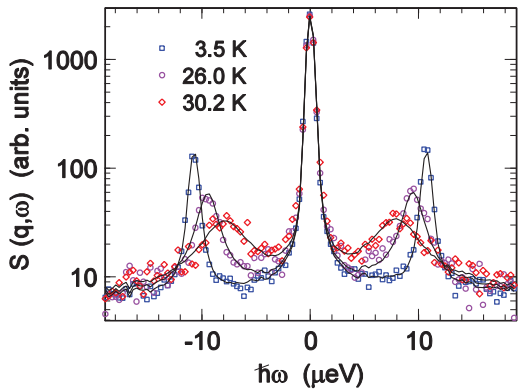

(a)

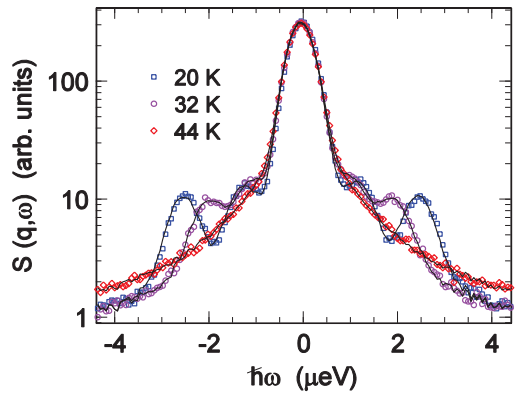

(b)

FIG. 3. Tunneling spectra (a) of 4,4′-dimethyl-2,2′-bipyridyl in the energy range ±14 μeV as well as (b) of its complex with chloranilic acid in the energy range ±4 μeV for several temperature between 3.5 and 40 K.

The estimate of the E_{01} value was made for the neutron spectra measured between 27.9 and 37.9 K. The tunneling frequencies for the compounds under investigation and the corresponding energies are collected in Table IV.

Because the peaks overlap one another as well as they are close to the central elastic peak, a quantitative analysis of line widths is practically impossible. We can state only that the intensities of two peaks in the case of the 4,4′-DMBP · CLA complex exhibit similar intensities and they correspond to two non-equivalent methyl groups in the crystal structure.

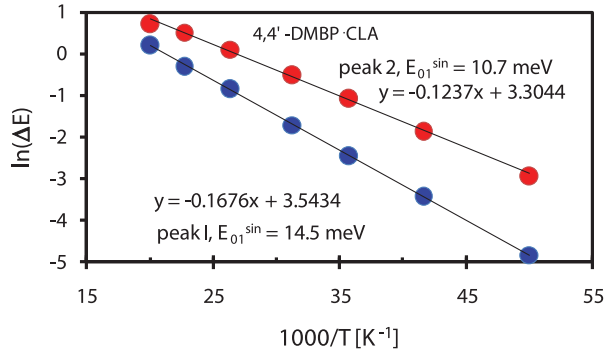

FIG. 4. Arrhenius plot ln(ΔE) *vs.* 1/*T* for 4,4′-dimethyl-2,2′-bipyridyl with CLA.

TABLE IV. Tunneling energies (μeV) for the dimethyl-2,2′-bipyridyls and their 1:1 complexes with chloranilic acid at 3.5 K and corresponding energies of activation estimated according to Eqs. (4).

	Pure	E_{01}^{sin} (meV)	In complex with chloranilic acid	E_{01}^{sin} (meV)
4,4′-dimethyl-2,2′-	10.5	13.0	1.0	14.5
bipyridyl			2.3	10.7
5,5′-dimethyl-2,2′-	1.4	10.6	Not observed	…
bipyridyl	13.1	6.31		
6,6′-dimethyl-2,2′-bipyridyl	1.1		Not observed	…

In all three cases, the complexation with CLA leads to a decrease of the electron density in the pyridine rings that should cause a drop of the potential barrier to the CH_3 group rotations. The results presented in this paper show the opposite effect – for the complex the tunneling peaks appear at lower energies in comparison to those for the pure 4,4′-dimethyl-2,2′-bipyridyl. This can be interpreted by envisaging that, in our case, a packing effect in the crystal lattice, leading to an increase in the barrier height, is more important. Further studies are needed to clarify more quantitatively the interplay of the two analyzed effects.

C. Thermal properties (TGA, DTA, DSC, and dilatometric) for 6,6′-DMBP · CLA

The preliminary thermal studies on 6,6′-DMBP · CLA showed that this complex undergoes a structural phase transition. This is a reason why we have undertaken the detailed investigation of its physical properties in a wide temperature range.

The thermal stability of 6,6′-DMBP · CLA was studied by means of simultaneous thermogravimetric analysis and differential thermal analysis between 290 and 700 K. The results presented in Fig. 5 indicate that 6,6′-DMBP · CLA is stable up to about 430 K. Above this temperature, the loss of weight exceeds 3%, which can be seen as the limit of thermal stability of the compound.

The results of the calorimetric measurements for 6,6′-DMBP · CLA are illustrated in Fig. 6. The DSC runs exhibit at 317/325 K on cooling/heating small changes in the heat flow, which are characteristic of a continuous transition. Although the measurements were carried out at different temperature rates, between 5 and 20 K/min., the small temperature hysteresis on cooling/heating was always observed. This observation may indicate the transition is only close to continuous. When the 6,6′-DMBP · CLA sample was cooled from room temperature down to 100 K, no phase transition was detected.

Figure 7 shows the results of the linear thermal expansion, $\Delta L/L_o$, measurements obtained along the ***a***-, ***b***-, and ***c***-axis (notation for the monoclinic system – phase $P2_1$) for the 6,6′-DMBP · CLA. The results obtained during heating and cooling circle are reversible and correspond to the phase transition at 317/325 K, found by the DSC technique.

The transformation at 317/325 K (on cooling/heating) in 6,6′-DMBP · CLA is accompanied by the $\Delta L/L_o$ change

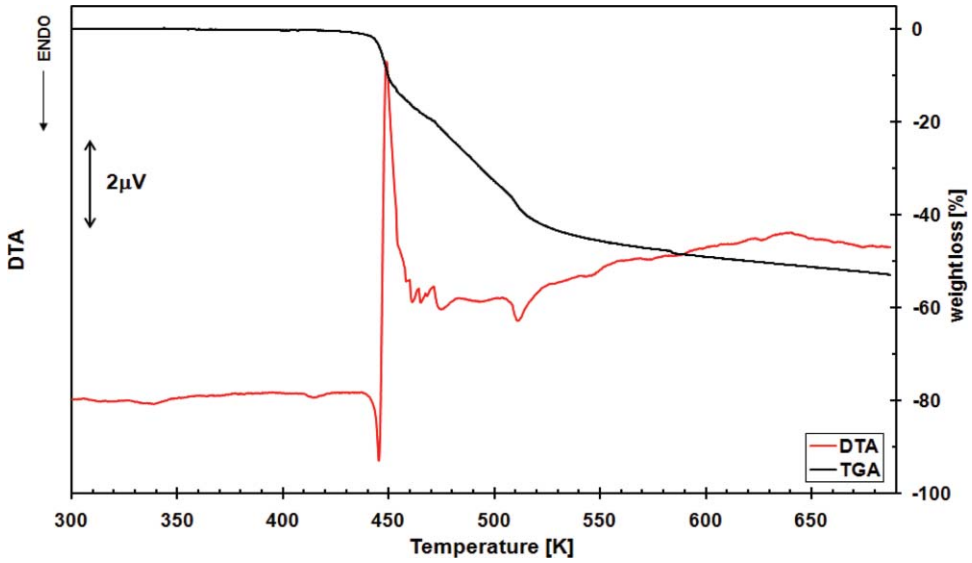

FIG. 5. Simultaneous DTA and TGA plots of the complex of 6,6′-dimethyl-2,2′-bipyridyl with CLA.

characteristic of a continuous transformation. No clear stepwise change in the value of the linear thermal expansion, $\Delta L/L_o$, at the phase transformation temperature is observed. Nevertheless, again a temperature hysteresis similar to that observed in the calorimetric results (see Figs. 6 and 7) was found, most probably related to the fact that a pure continuous transition is not occurring. One cannot, however, exclude that the temperature hysteresis is an artefact in some way related to the relatively large dimensions of the low heat conductivity single crystal samples.

On the basis of the dilatometric results, one can state that the dimensions of the crystal along the ***a***- and ***c***-direction diminish, whereas along the ***b***-direction it increases. The effects corresponding to the phase transition at 317/325 K are characteristic of the continuous transitions – only a continuous change of the value of thermal coefficient of the linear expansion, $\alpha = \Delta L/L_o \Delta T$, is observed.

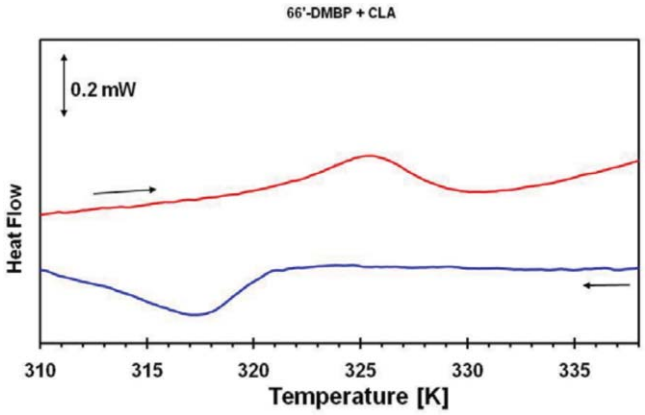

FIG. 6. The results of the DSC calorimetric measurements for 6,6′-dimethyl-2,2′-bipyridyl with CLA during heating and cooling runs (20 K/min, m = 10 mg).

D. Dielectric properties

The purpose of the dielectric measurements of 6,6′-DMBP · CLA was to determine the nature of the phase

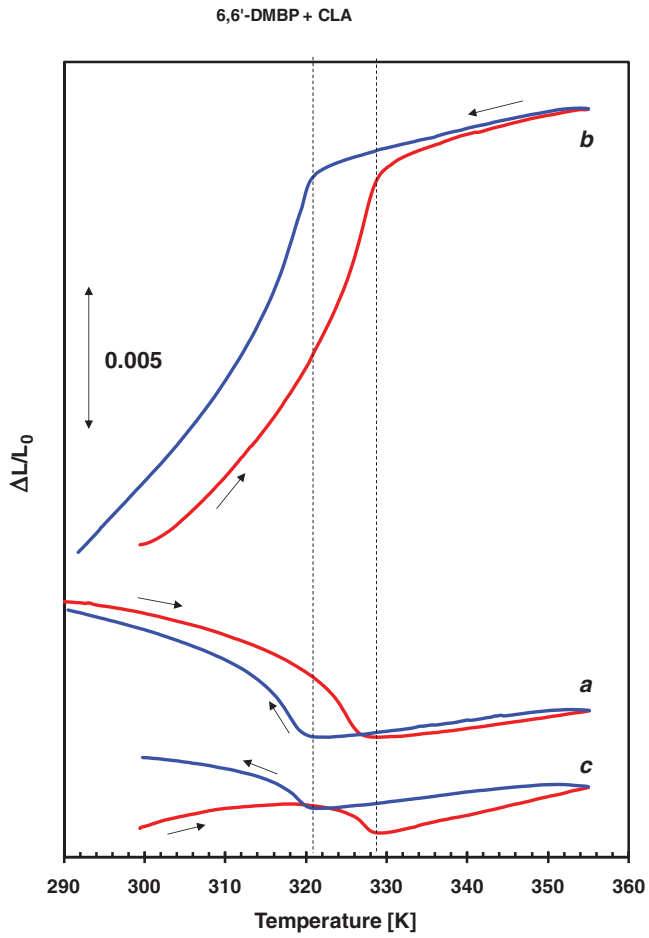

FIG. 7. The temperature dependence of the linear thermal expansion, $\Delta L/L_o$, obtained along the ***a***-, ***b***-, and ***c***-axis (notation for the monoclinic system – phase $P2_1$) for the 6,6′-dimethyl-2,2′-bipyridyl with CLA complex. (Thickness of the lines corresponds to the measurement error.)

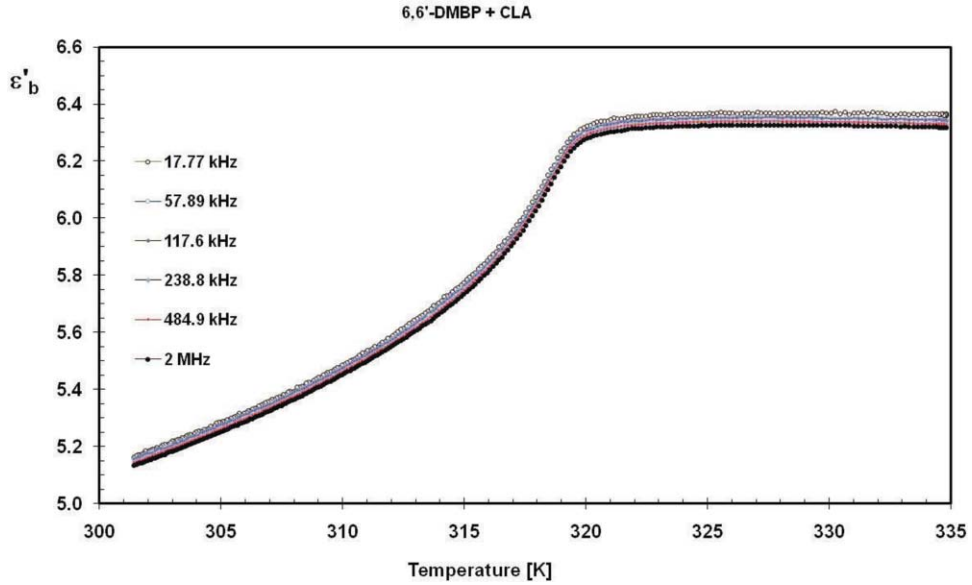

FIG. 8. The temperature dependence of the real part of the electric permittivity, ε'_b along the ***b***-axis for the selected frequencies.

transition at 317 K and to detect the possible molecular dynamics in the single crystals. For 6,6′-DMBP · CLA, we carried out the measurements of the complex electric permittivity, $\varepsilon^* = \varepsilon' - i\varepsilon''$, as a function of temperature (between 300 and 330 K) and frequency (between 30 kHz and 2 MHz) along the polar ***b***-direction.

The temperature dependence of the real part of the electric permittivity, ε'_b along the ***b***-axis for the selected frequencies is presented in Fig. 8. The measurements were carried out during a cooling scan. The runs obtained during heating scans are reversible; however, a small temperature hysteresis is still observed. The temperature range chosen for the dielectric measurements corresponds to that of the phase transitions detected by the DSC and dilatometric techniques. Generally, one can state that the observed temperature dependence of the ε'_b value, although found at the same temperature as in the DSC and dilatometric experiments, is rather weak ($\Delta\varepsilon \approx 1.2$). In these types of compounds, it may be assigned to small changes in the unit cell dipole moment under the ac electric field. It is clearly seen that above 320 K the electric permittivity is larger than that in the low-temperature phase and that below ~317 K it continuously decreases. This behavior on cooling may indicate that the motions of molecules, which are responsible for the enhanced value of the electric permittivity in the high-temperature phase, continuously freeze.

Taking into account that the dimension of the crystal diminishes along the ***b***-direction, which should result in an increase in polarizability along this direction, the observed opposite change in the electric permittivity value indicates the freezing of some molecular dynamics in the low-temperature phase. It is probably related to a gradual limitation of the proton motional freedom in the hydrogen bonds. The small value of the permittivity excludes a long-range interaction and consequently the appearance of the antiferroelectric ordering. This observation indicates an essential difference between the 6,6′-DMBP · CLA described in this paper and the 5,5′-DMBP · CLA described by Kumai *et al.*[3]

The value of the real electric permittivity, ε'_b, is practically independent of frequency, the observed differences at the particular frequencies is probably related to the measuring error. Moreover, there is no change in the value of the imaginary part of permittivity, ε''_b, in the temperature and frequency ranges applied. This indicates that there is no dielectric relaxation process observed in this frequency range along the crystallographic ***b***-direction. We deduce, therefore, that the molecular motion, which corresponds to the enhanced ε'_b value in the phase above 320 K, is most probably too fast to be detected by these frequencies.

E. IR and Raman spectroscopy

The IR and Raman spectra between 3500 and 100 cm^{-1} of 4,4′-DMBP · CLA, 5,5′-DMBP · CLA, and 6,6′-DMBP · CLA at 300 K are presented in Figs. 9(a)–9(c). The assignments of the observed bands in the IR and Raman spectra were made on the basis of calculation performed for the 4,4′- and 5,5′-dimethyl-2,2′-bipyridyl with squaric acid complexes.[2]

Looking at the spectra shown in Figs. 9(a)–9(c), the continua assigned to the stretching vibrations of N^+–H and OH groups engaged in strong hydrogen bonds seem most characteristic. The continua can be interpreted in terms of the excited state double-well energy model for the proton in the hydrogen bond.[23] In the case of the 5,5′-dimethyl derivative, the continua are spread in the range starting at ~3000 cm^{-1} down to ~400 cm^{-1}. In this case, the hydrogen bonds are the shortest and the continuum reaches the smallest wavenumber. For the remaining derivatives, the continua are spread to ~700 cm^{-1}. More precise analysis is not possible, because in all cases an overlapping of bands ascribed to N^+–H · · · O^- and O–H · · · N bridges takes place.

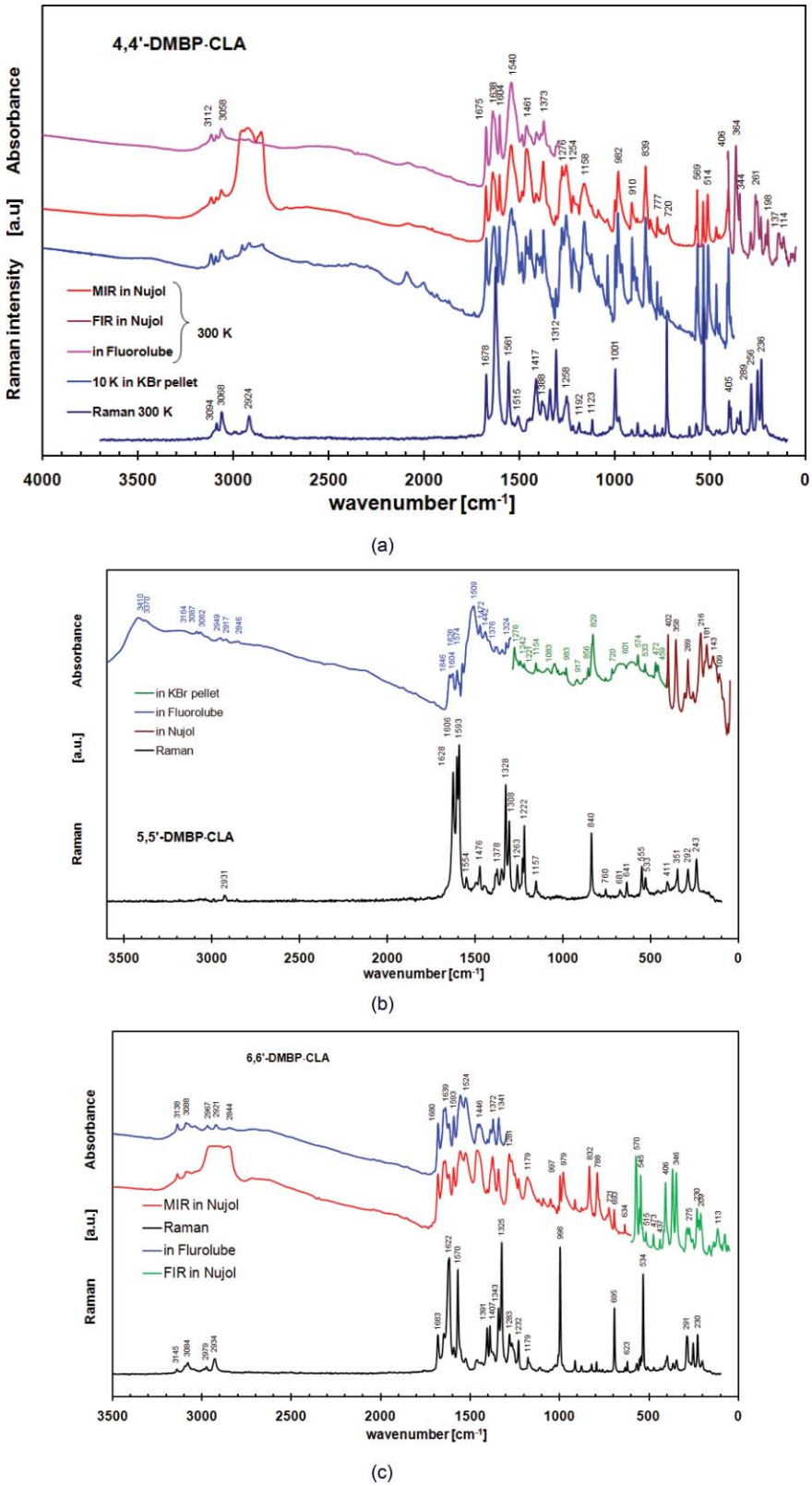

FIG. 9. The IR and Raman spectra between 3500 and 100 cm^{-1} of (a) 4,4′-, (b) 5,5′-, and (c) 6,6′-dimethyl-2,2′-bipyridyl complexes with CLA at 300 K.

As far as the deformation δ(NH) and δ(OH) vibrations are concerned, we observe bands at frequencies 1680 and 1639 cm^{-1} for 6,6′-dimethyl derivative, 1675 and 1638 cm^{-1} for 4,4′-dimethyl derivative, and 1646 and 1628 cm^{-1} for 5,5′-dimethyl derivative, which possesses the shortest hydrogen bonds. With respect to the vibration of CH_3 and C–H groups in the pyridyl rings, the stretching modes for all three derivatives are similar. Thus, one observes two triplets above and below 3000 cm^{-1}. Their behavior is presented in Fig. 10, which illustrates the evolution of those bands at low temperatures.

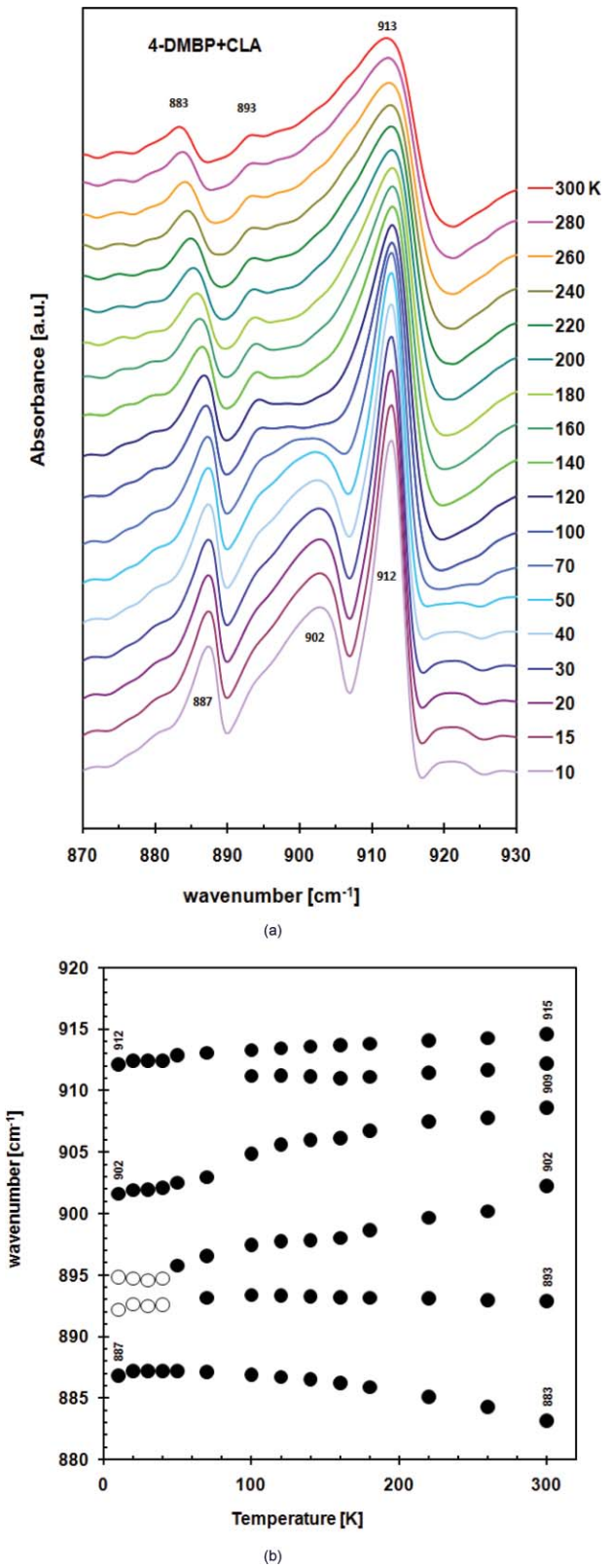

FIG. 10. (a) Infrared spectra for 4,4′-dimethyl-2,2′-bipyridyl with CLA between 850 and 950 cm^{-1} assigned to the CH_3 deformation vibrations at the selected temperatures (10–300 K). (b) Temperature dependencies of the frequencies of some selected bands from the region between 2800 and 3200 cm^{-1} for 4,4′-dimethyl-2,2′-bipyridyl complex with CLA.

Finally, we would like to draw attention to the intense band in the region 830–840 cm^{-1} ascribed to the γ(CH) vibration of the pyridyl moieties. The δ(CH) vibrations are not characteristic because they are mixed with modes ascribed to the stretching vibration of the rings. The triplets of $\nu(CH_3)$ and ν(C–H) vibrations are not meaningful with the exception of some bands assigned to the CH_3 groups. An additional weak band at 2870 cm^{-1} and the splitting of the band at 2850 cm^{-1} appear. This phenomenon is connected with the rotation of the methyl groups that find a reflection in tunneling splitting.

The infrared spectra for one of the complexes, namely, for 4,4′-dimethyl-2,2′-bipyridyl with CLA, have been recorded between 3500 and 400 cm^{-1} at selected temperatures between 10 and 300 K. The main purpose of these investigations was to gain more information about the lowest temperature region, in which the tunneling of the CH_3 groups has been observed in the neutron scattering spectra. The observation may be based on the fact that the dynamical state of the molecule affects the positions and shapes of bands assigned to the internal vibrations of the cations.

On heating the sample from 10 to 300 K, remarkable changes are observed at wavenumbers between 950 and 850 cm^{-1}. The temperature evolution of the bands in the infrared spectra for 4,4′-dimethyl-2,2′-bipyridyl with CLA in this frequency region assigned to the CH_3 deformation vibrations are presented in Fig. 10(a). In turn, the temperature dependencies of some other selected bands are depicted in Fig. 10(b). One can state that real changes in the band positions (e.g., for bands at 887 and 902 cm^{-1}, 10 K) have occurred. The most remarkable of these are observed for the bands between 890 and 900 cm^{-1} for temperatures below ~100 K. The changes are very small, but they are undoubtedly above the error of the estimation of these positions. The most significant changes, however, are observed for the intensities for the bands appearing between 890 and 900 cm^{-1}.

IV. CONCLUSIONS

The motivation of these studies was the fact that 5,5′-DMBP complexed with chloranilic acid shows an antiferroelectric proton mediated phase transition.[3] It was shown that the polar properties of 5,5′-DMBP · CLA are related to the proton dynamics – motion of the protons is possible only in the hydrogen bonds – the remaining structure is rather rigid. Moreover, a strong isotopic effect was found associated with the temperature of the antiferroelectric phase transition. In all cases presented in the present paper, i.e., 4,4′-DMBP · CLA, 5,5′-DMBP · CLA, and 6,6′-DMBP · CLA, the hydrogen bonded chains are formed with the OH group of chloranilic acid ionized via the proton transfer, $N^+H\cdots O^-$. The other hydrogen bond formed between the bipyridyl and CLA is an ordinary $OH\cdots N$ bridge. The analysis of hydrogen bonds in all three derivatives shows that the shortest H-bond is present in the complex of 5,5′-dimethyl derivative, while the longest one is in the 6,6′-derivative (see Table III). This undoubtedly leads to an increase of electric permittivity at the phase transition in 5,5′-DMBP · CLA. In the case of 6,6′-DMBP · CLA, one observes also the close to continuous

phase transition at ~320 K that was the object of our detailed studies using DSC, dilatometric, and dielectric techniques. The dilatometric measurement performed with the single crystal has shown that the $\Delta L/L_o$ value is the highest along the ***b***-axis, which is consistent with the direction of the hydrogen bonded chains. The jump of dielectric permittivity at the transition point is, however, small (~1.2, in comparison to 150 for 5,5′-DMBP · CLA) and can be ascribed to a diminishing polarizability of hydrogen bridges on crossing the phase transition at 320 K, when the sample is cooled. It does not lead, however, to the long range interactions as in the ferroelectric or antiferroelectric crystals. Using the DSC technique down to 100 K as well as the infrared spectra down to 10 K, no substantial changes, which might have been assigned to structural phase transition, were detected for 6,6′-DMBP · CLA. This means that the supramolecular structure of hydrogen bonded chains does not change in this temperature interval. It indicates also that the crystal structure at 100 K and at room temperature is the same. To gain more information about the proton dynamics in the high-temperature phase, above ~320 K, additional measurements should be undertaken, e.g., solid state NMR on the deuterated sample should be applied.

For several years, we have carried out systematic studies on tunneling splittings in methyl derivatives as components in molecular complexes.[16,24,25] We expect that the energy of tunnel splitting together with activation energy obtained from the quasi-elastic neutron scattering and the energy of the torsional vibrations of the methyl groups will be a measure of the charge transfer between molecules in the complexes. In this work, high resolution tunneling spectra have been recorded for neat dimethyl derivatives and their complexes with chloranilic acid. The splitting is observed in all three neat components and only in one complex formed by the 4,4′-dimethyl derivative. No regular features were, however, found with respect to the tunneling splitting but one can suppose that the most important factor is the crystal packing affecting the dynamics of methyl groups. In complexes with chloranilic acid, the tunneling splitting is not observed ($\hbar\omega$ may be less than 1 μeV) or it is very small in the case of the 4,4′-derivative. The formation of complexes with chloranilic acid leads to an intensification of the potential and the methyl groups are sensitive to this barrier increase. The charge distribution in the complex, altered by hydrogen bond formation, should cause a drop of the rotational potential, which is not observed. In the case of the decrease of the potential the energy of the CH_3 group, tunneling should remarkably increase.

The analysis of infrared spectra of the three complexes of bipyridyls allows us to draw the following conclusions. The most characteristic feature seems to be a display of absorption continua in the wavenumber range 500–3000 cm^{-1}, which is of low intensity compared with many other strong OH · · · N hydrogen bonds. The quantitative analysis of absorption is not possible because of the overlapping absorptions assigned to $\nu(N^+H)$ and ν(OH) modes. The temperature dependence of ν(CH) modes of methyl groups indicates clearly some changes including the splitting and shift of some bands which can be attributed to the rotation of methyl groups.

ACKNOWLEDGMENTS

This work was supported by the Polish Ministry of Science and Higher Education (Project Register No. N N204 2497 34) and partially by the International Programme ZIBJ DUBNA 04-4-1069-2009/2010.04.29 (Decision No. 868/W-ZIBJ DUBNA/2010/0). This research project has been supported by the European Commission under the 7th Framework Programme through the Key Action: Strengthening the European Research Area, Research Infrastructures (Contract No. 226507 (NMI3)).

[1] D. M. S. Martins, D. S. Middlemiss, C. R. Pulham, C. C. Wilson, M. T. Weller, P. F. Henry, N. Shankland, K. Shankland, W. G. Marshal, R. M. Ibberson, K. Knight, S. Moggach, M. Brunelli, and C. A. Morrison, J. Am. Chem. Soc. **131**, 3884 (2009).
[2] J. Nowicka-Scheibe, E. Grech, W. Sawka-Dobrowolska, G. Bator, A Pawlukojć, and L. Sobczyk, J. Mol. Struct. **976**, 30 (2010).
[3] R. Kumai, S. Horiuchi, Y. Okimoto, and Y. Tokura, J. Chem. Phys. **125**, 084715 (2006).
[4] S. Horiuchi, R. Kumai, and Y. Tokura, Angew. Chem., Int. Ed. **46**, 3497 (2007).
[5] S. Horiuchi and Y. Tokura, Nature Mater. **7**, 357 (2008).
[6] S. Horiuchi, F. Ishii, R. Kumai, Y. Okimoto, H. Tachibana, H. Nagaosa, and Y. Tokura, Nature Mater. **4**, 163 (2005).
[7] S. Horiuchi, R. Kumai, and Y. Tokura, J. Am. Chem. Soc. **127**, 5010 (2005).
[8] M. Prager, A. Pietraszko, L. Sobczyk, A Pawlukojć, E. Grech, T. Seydel, A. Wischnewski, and M. Zamponi, J. Chem. Phys. **125**, 194525 (2006).
[9] M. Prager, W. Sawka-Dobrowolska, L. Sobczyk, A Pawlukojć, E. Grech, A. Wischnewski, and M. Zamponi, Chem. Phys. **332**, 1 (2007).
[10] H. Suzuki, H. Mori, J.-I. Yamaura, M. Matsuda, H. Tajima, and T. Mochida, Chem. Lett. **36**, 402 (2007).
[11] S. Horiuchi, R. Kumai, Y. Tokunaga, and Y. Tokura, J. Am. Chem. Soc. **130**, 13382 (2008).
[12] M. Plazanet, M. R. Johnson, J. D. Gale, T. Yildirin, G. J. Kearley, M. T. Fernandez-Diaz, D. Sanchez-Portal, E. Artacho, J. M. Soler, P. Ordejon, A. Garcia, and H. P. Trommsdorff, Chem. Phys. **261**, 189 (2000).
[13] G. Bator, L. Sobczyk, A. Pawlukojć, J. Nowicka-Scheibe, E. Grech, J. Krawczyk, M. Nowina-Konopka, I. Natkaniec, I. V. Kalinin, and O. Steinsvoll, Phase Transitions **80**, 489 (2007).
[14] A. Pawlukojć, I. Natkaniec, G. Bator, L. Sobczyk, E. Grech, and J. Nowicka-Scheibe, Spectrochim. Acta, Part A **63**, 766 (2006).
[15] W. Sawka-Dobrowolska, G. Bator, B. Czarnik-Matusewicz, L. Sobczyk, A. Pawlukojć, J. Nowicka-Scheibe, E. Grech, and H. Rundlof, Chem. Phys. **327**, 237 (2006).
[16] M. Prager, A. Pawlukojć, L. Sobczyk, E. Grech, and H. Grimm, J. Phys. Condens. Matter **17**, 5725 (2005).
[17] M. Prager, A. Wischnewski, G. Bator, E. Grech, A. Pawlukojć, and L. Sobczyk, Chem. Phys. **334**, 148 (2007).
[18] G. M. Sheldrick, SHELXS-97, a program for solution of crystal structure, University of Göttingen, Germany, 1997; SHELXL-97, a program for structure refinement of crystal structures, University of Göttingen, Germany, 1997.
[19] See http://www.jcns.info/jcns_spheres. The website provides information about the SPHERES, a third-generation backscattering neutron spectrometer.
[20] W. Press, *Single-Particle Rotations in Molecular Crystals*, Springer Tracts in Modern Physics Vol. 92 (Springer-Verlag, Berlin, 1981).
[21] M. Prager and A. Heidemann, Chem. Rev. **97**(8), 2933 (1997).
[22] O. Kirstein, M. Prager, and G. J. Schneider, J. Chem. Phys. **130**, 214508 (2009).
[23] Z. Mielke and L. Sobczyk, in *Isotope Effects in Chemistry and Biology*, edited by A. Kohen and H.-H. Limbach (CRC, Boca Raton, 2006), p. 281.
[24] M. Prager, A. Pietraszko, L. Sobczyk, A. Pawlukojć, E. Grech, T. Seydel, A. Wischnewski, and M. Zamponi, J. Chem. Phys. **125**, 194525 (2006).
[25] W. Sawka-Dobrowolska, G. Bator, L. Sobczyk, E. Grech, J. Nowicka-Scheibe, A. Pawlukojć, and J. Wuttke, J. Mol. Struct. **975**, 298 (2010).
[26] Copies of this information may be obtained free of charge from the Director, CCDC, 12 Union Road, Cambridge CB2 1EZ, UK. Fax: +44-1223-336033; e-mail: deposit@ccdc.cam.ac.uk or http://www.ccdc.cam.ac.uk.